

## Electromagnetic Form Factors of Charged and Neutral Kaons

C. J. Burden\*, C. D. Roberts†, and M. J. Thomson‡

\**Department of Theoretical Physics, Research School of Physical Sciences and Engineering,  
Australian National University, Canberra ACT 0200, Australia*

†*Physics Division, Bldg. 203, Argonne National Laboratory, Argonne IL 60439-4843*

‡*School of Physics, University of Melbourne, Parkville VIC 3052, Australia*

(24/10/95)

### Abstract

The charged and neutral kaon form factors are calculated as a phenomenological application of the QCD Dyson-Schwinger equations. The results are compared with the pion form factor calculated in the same framework and yield  $F_{K^\pm}(Q^2) > F_{\pi^\pm}(Q^2)$  on  $Q^2 \in [0, 3]$  GeV<sup>2</sup>; and a neutral kaon form factor that is similar in form and magnitude to the neutron charge form factor. These results are sensitive to the difference between the kaon and pion Bethe-Salpeter amplitude and the  $u$ - and  $s$ -quark propagation characteristics.

PACS NUMBERS: 13.40.Gp, 14.40.Aq, 12.38.Lg, 24.85.+p

KEYWORDS: Hadron Physics  $F_{K^\pm}(Q^2)$ ,  $F_{K^0}(Q^2)$ ,  $F_{\pi^\pm}(Q^2)$ ; Dyson-Schwinger Equations; effects of quark and gluon confinement; nonperturbative QCD phenomenology.

**1. Introduction.** The kaon is the simplest strangeness-carrying bound state. Hence studies of kaon observables and their comparison with analogous pion properties provide information about  $SU_f(3)$ -breaking in QCD. Particularly interesting are nonperturbative effects, defined as those whose source is the difference  $m_s - m_u$  but which cannot simply be described as a linear response to this difference. Examples are the difference between the kaon and pion Bethe-Salpeter amplitude and that between the  $u$ - and  $s$ -quark propagation characteristics at small and intermediate  $k^2$ ; i.e.,  $k^2 \in [0, 1 \sim 2] \text{ GeV}^2$ , both of which are generated nonperturbatively.

The electromagnetic form factors of the charged and neutral kaon are sensitive to these effects and are accessible to experiments at CEBAF [1]. Herein we report a calculation of a range of pion and kaon observables via a semi-phenomenological application of the Dyson-Schwinger equations (DSEs) [2] in QCD; our primary focus being the elastic charged and neutral kaon form factors. In calculating these form factors we employ a generalised-impulse approximation, in which the quark propagators (2-point Schwinger functions), meson Bethe-Salpeter amplitudes (meson-quark vertices) and quark-photon vertices are dressed quantities whose form follows from nonperturbative, semi-phenomenological DSE studies in QCD [2]. In this way our calculation provides for an extrapolation of the known large spacelike- $k^2$  behaviour of these Schwinger functions to the small spacelike- $k^2$  region, where they are unknown and confinement effects are manifest. This facilitates an exploration of the relationship between physical observables and the nonperturbative, infrared behaviour of these Schwinger functions.

This calculation is a recapitulation, reanalysis and extension of the study of the pion presented in Ref. [3]. In this approach the quark propagator has no Lehmann representation and hence may be interpreted as describing a confined particle since this feature is sufficient to ensure the absence of quark production thresholds in  $S$ -matrix elements describing colour-singlet to singlet transitions. The quark-photon vertices, which describe the coupling of a photon to the dressed  $u$ - and  $s$ -quarks, follow from extensive QED studies [4] and satisfy the Ward-Takahashi identity. This necessarily entails that the  $\gamma$ - $K$ - $K$  and  $\gamma$ - $\pi$ - $\pi$  amplitudes are current conserving. In the chiral limit the quark-pseudoscalar vertex is completely determined by the scalar part of the quark self-energy [5], which is a manifestation of Goldstone's theorem in the DSE approach. The extension to finite quark masses requires a minimal modification and preserves Dashen's relation [6].

**2. Generalised Impulse Approximation to  $F_K(Q^2)$ .** In Euclidean space, with metric  $\delta_{\mu\nu} = \text{diag}(1, 1, 1, 1)$ ,  $\gamma_\mu = \gamma_\mu^\dagger$  and  $\{\gamma_\mu, \gamma_\nu\} = 2\delta_{\mu\nu}$ , the generalised impulse approximation to the  $\gamma$ - $K^+$ - $K^-$  vertex is given by

$$\Lambda_\mu^{K^\pm}(p, -q) = \frac{2}{3}\Lambda_\mu^u(p, -q) + \frac{1}{3}\bar{\Lambda}_\mu^s(p, -q) \quad (1)$$

where

$$\Lambda_\mu^u(p, -q) = 2N_c \int \frac{d^4k}{(2\pi)^4} \text{tr}_D[\bar{\Gamma}_K(k; p) S_u(k + \alpha p) i\Gamma_\mu^u(k + \alpha p, k - \beta p + q) \times \quad (2)$$

$$S_u(k - \beta p + q) \Gamma_K(k - \beta(p - q); -q) S_s(k - \beta p)],$$

$$\bar{\Lambda}_\mu^s(p, -q) = 2N_c \int \frac{d^4k}{(2\pi)^4} \text{tr}_D[\Gamma_K(k; p) S_s(k + \beta p) i\Gamma_\mu^s(k + \beta p, k - \alpha p + q) \times \quad (3)$$

$$S_s(k - \alpha p + q) \bar{\Gamma}_K(k - \alpha(p - q); -q) S_u(k - \alpha p)].$$

Here  $q$  is the initial momentum of the kaon,  $p - q \equiv Q$  is the photon momentum and only the Dirac trace remains to be evaluated. In Eqs. (2) and (3):  $S_f$  is the propagator for a quark of flavour  $f = u, s$ ;  $\Gamma_K(p; P)$  is the kaon Bethe-Salpeter amplitude, with quark-antiquark relative momentum  $p$  and centre-of-mass momentum  $P$ ; and  $\Gamma_\mu^f$  is the flavour dependent photon-quark vertex. The parameter  $\alpha$  [ $\beta = 1 - \alpha$ ] allows for uneven partitioning of the total momentum between the  $u$ - and  $s$ -quark legs connected to the Bethe-Salpeter amplitude and is fixed by requiring  $F_{K^0}(Q^2 = 0) = 0$ . The first of the two contributions in Eq. (1) corresponds to the  $u$ -quark interacting with the photon and the  $s$ -quark acting as a spectator; in the second the roles are reversed.

If the quark masses are set equal in Eq. (1) the generalised impulse approximation to the  $\gamma$ - $\pi$ - $\pi$  vertex [3,7] is recovered, provided that  $\Gamma_K \rightarrow \Gamma_\pi$ ,  $f_K \rightarrow f_\pi$  and  $\alpha = 1/2$ , which is required by charge conjugation symmetry.

The generalised impulse approximation to the neutral-kaon-photon vertex is given by

$$\Lambda_\mu^{K^0}(p, -q) = -\frac{1}{3}\Lambda_\mu^d(p, -q) + \frac{1}{3}\bar{\Lambda}_\mu^s(p, -q). \quad (4)$$

Herein, except for the electric charge, the  $u$  and  $d$  quarks are identical and hence  $\Lambda_\mu^d(p, -q) = \Lambda_\mu^u(p, -q)$ , defined in Eq. (2).

For elastic scattering [ $p^2 = q^2$ ] and  $\Lambda_\mu^{K^\pm/K^0}(p, -q) = (p + q)_\mu F^{K^\pm/K^0}(Q^2)$ , where  $F^{K^\pm/K^0}(Q^2)$  is the electromagnetic form factor.

**2.1 Dressed quark propagator.**  $S_f = -i\gamma \cdot p \sigma_V^f(p^2) + \sigma_S^f(p^2)$  in Eqs. (2) and (3) can be obtained by solving the quark Dyson-Schwinger equation [2]. Realistic, semi-phenomenological studies provide the basis for the following *approximating* algebraic, model forms for  $\sigma_V^f$  and  $\sigma_S^f$  [3]:

$$\bar{\sigma}_S^f(x) = C_{\bar{m}_f}^f e^{-2x} \quad (5)$$

$$+ \frac{1 - e^{-b_1^f x}}{b_1^f x} \frac{1 - e^{-b_3^f x}}{b_3^f x} \left( b_0^f + b_2^f \frac{1 - e^{-\Lambda x}}{\Lambda x} \right) + \frac{\bar{m}_f}{x + \bar{m}_f^2} \left( 1 - e^{-2(x + \bar{m}_f^2)} \right),$$

$$\bar{\sigma}_V^f(x) = \frac{2(x + \bar{m}_f^2) - 1 + e^{-2(x + \bar{m}_f^2)}}{2(x + \bar{m}_f^2)^2} - \bar{m}_f C_{\bar{m}_f}^f e^{-2x}, \quad (6)$$

where ( $x = y^2 = p^2/\sqrt{2D}$ ) and:  $\bar{\sigma}_V(y^2) = 2D \sigma_V(p^2)$ ;  $\bar{\sigma}_S(y^2) = \sqrt{2D} \sigma_S(p^2)$ ; and  $\bar{m}_f = m_f/\sqrt{2D}$ , with  $D$  a mass scale. The parameters  $C_{\bar{m}_f}^f$ ,  $\bar{m}_f$ ,  $b_{1...3}^f$  are determined either by: 1) fitting a quark-DSE solution obtained with a realistic gluon propagator; or 2) performing a  $\chi^2$ -fit to a range of hadronic observables. ( $\Lambda = 10^{-4}$  is included to decouple the small and large spacelike- $p^2$  behaviour of the  $1/p^4$  term, characterised by  $b_0^f$  and  $b_2^f$ .) We write the inverse of the quark propagator as

$$S_f^{-1}(p) = i\gamma \cdot p A^f(p^2) + B^f(p^2). \quad (7)$$

The quark propagator described by Eqs. (5)-(6) is an entire function in the finite complex- $p^2$  plane and hence does not have a Lehmann representation. It therefore admits the interpretation that it describes a confined particle [2]. The  $\sim e^{-x}$  form that ensures this is suggested by the algebraic solution of the model DSE studied in Ref. [9], which employed a confining model gluon propagator and dressed quark-gluon vertex.

The behaviour of this model form on the spacelike- $p^2$  axis is such that, neglecting  $\ln[p^2]$  corrections associated with the anomalous dimension of the quark propagator in QCD, it manifests asymptotic freedom. It has a term associated with dynamical chiral symmetry breaking ( $\sim 1/x^2$ ) and a term associated with explicit chiral symmetry breaking ( $\sim m/x$ ). Both of these terms are present in solutions of the quark DSE using a realistic model gluon propagator [10].

**2.2 Pseudoscalar Meson Bethe-Salpeter Amplitude.**  $\Gamma_K$  in Eq. (1) is the solution of an homogeneous Bethe-Salpeter equation (BSE). Many studies of this BSE suggest strongly that the amplitude is  $\propto \gamma_5$ . Furthermore, in the chiral limit the pseudoscalar BSE and quark DSE are identical [5] and one has a massless excitation in the pseudoscalar channel with  $\Gamma_{\text{pseudoscalar}}(p; P^2 = 0) = i\gamma_5 B_{m=0}(p^2)/f_\pi$ , where  $B_{m=0}(p^2)$  is given in Eq. (7) with  $m_f = 0$ . This is the realisation of Goldstone's theorem in the DSE framework; i.e., in the chiral limit Eqs. (5) and (6) completely determine  $\Gamma_{\text{pseudoscalar}}$ .

Herein, based on these observations, we employ the approximations

$$\Gamma_\pi(p; P^2 = -m_\pi^2) \approx i\gamma_5 \frac{1}{f_\pi} B_{m_u=0}^u(p^2), \quad (8)$$

$$\Gamma_K(p; P^2 = -m_K^2) \approx i\gamma_5 \frac{1}{f_K} B_{m_s=0}^s(p^2). \quad (9)$$

For the pion this is a good approximation, both pointwise and in terms of the values obtained for physical observables [11]. For the kaon it is an exploratory Ansatz, one which need only be accurate as an approximation to the integrated strength.

**2.3 Quark-photon Vertex.**  $\Gamma_\mu^f(p_1, p_2)$  in Eq. (1) satisfies a DSE that describes both strong and electromagnetic dressing of the quark-photon vertex. Solving this equation is a difficult problem that has only recently begun to be addressed [12]. However, much progress has been made in developing a realistic Ansatz for  $\Gamma_\mu(p_1, p_2)$  [4]. The bare vertex,  $\Gamma_\mu(p_1, p_2) = \gamma_\mu$ , is inadequate when the fermion 2-point Schwinger function has momentum dependent dressing because it violates the Ward-Takahashi identity. In Ref. [13] the following form was proposed

$$\Gamma_\mu^f(p, k) = \Sigma_A^f(p^2, k^2) \gamma_\mu + (p+k)_\mu \left[ \frac{1}{2} \gamma \cdot (p+k) \Delta_A^f(p^2, k^2) - i \Delta_B^f(p^2, k^2) \right], \quad (10)$$

with  $\Sigma_A^f(p^2, k^2) = [A^f(p^2) + A^f(k^2)]/2$ ,  $\Delta_A^f(p^2, k^2) = [A^f(p^2) - A^f(k^2)]/[p^2 - k^2]$  and  $\Delta_B^f(p^2, k^2) = [B^f(p^2) - B^f(k^2)]/[p^2 - k^2]$ . This Ansatz is *completely determined* by the dressed quark propagator; satisfies the Ward-Takahashi identity; has a well defined limit as  $p^2 \rightarrow k^2$ ; transforms correctly under  $C$ ,  $P$ ,  $T$  and Lorentz transformations; and reduces to the bare vertex in the manner prescribed by perturbation theory. Furthermore, it is relatively simple and hence an ideal form to be employed in our phenomenological studies.

Using charge conjugation it is straightforward to show that for elastic scattering one has  $(p-q)_\mu \Lambda_\mu^{K^{\pm,0}}(p, -q) = 0$  in generalised impulse approximation. The result  $F^{K^\pm}(-m_K^2, Q^2 = 0) = 1$  follows because the quark-photon vertex satisfies the Ward identity.

### 3. Calculated Spacelike Kaon Form Factors.

In the Breit frame:  $p = (0, 0, \frac{1}{2}Q, iE_K)$ ,  $q = (0, 0, -\frac{1}{2}Q, iE_K)$ ,  $E_K = \sqrt{(m_K^2 + Q^2)/4}$ ; the calculation of each meson form factor involves the numerical evaluation of a three-dimensional integral via straightforward numerical quadrature.

To fix the parameters in the quark propagators we have revised the study of Ref. [3] and refitted the pion observables using the pion mass formula described in Ref. [11]:

$$m_\pi^2 f_\pi^2 = \frac{N_c}{2\pi^2} \int_0^\infty ds s \frac{B_{\bar{m}_u=0}^u(s)}{B_{\bar{m}\neq 0}^u(s)} \left( B_{\bar{m}_u\neq 0}^u(s) \sigma_{S_{\bar{m}_u=0}}^u(s) - B_{\bar{m}_u=0}^u(s) \sigma_{S_{\bar{m}_u\neq 0}}^u(s) \right) , \quad (11)$$

$$f_\pi^2 = \frac{N_c}{8\pi^2} \int_0^\infty ds s \left[ B_{\bar{m}_u=0}^u(s) \right]^2 \left\{ (\sigma_V^u)^2 - 2 [\sigma_S^u \sigma_S^{u'} + s \sigma_V^u \sigma_V^{u'}] - s [\sigma_S^u \sigma_S^{u''} - (\sigma_S^{u'})^2] - s^2 [\sigma_V^u \sigma_V^{u''} - (\sigma_V^{u'})^2] \right\} . \quad (12)$$

with  $\sigma_V^u \equiv \sigma_{V_{\bar{m}_u\neq 0}}^u$  and  $\sigma_S^u \equiv \sigma_{S_{\bar{m}_u\neq 0}}^u$ . This mass formula yields an accurate estimate of the mass obtained by solving the generalised-ladder approximation to the pion Bethe-Salpeter equation [11].

This reanalysis, carried out with the constraint  $C_{\bar{m}_u\neq 0}^u = 0$ , leads to

$$\begin{aligned} C_{\bar{m}_u=0}^u &= 0.121, \quad \bar{m}_u = 0.00897, \\ b_0^u &= 0.131, \quad b_1^u = 2.90, \quad b_2^u = 0.603, \quad b_3^u = 0.185 \end{aligned} \quad (13)$$

with the mass scale  $D = 0.160$  GeV<sup>2</sup> chosen so as to give  $f_\pi = 92.4$  MeV. Table I provides a comparison between calculation and experiment.

**3.1 Differences between  $u$ - and  $s$ -quark propagators.** Based on the studies of Ref. [20] we set

$$\bar{m}_s = 12.5 (\bar{m}_u + \bar{m}_d) \equiv 25 \bar{m}_{\text{ave}} , \quad (14)$$

where  $\bar{m}_u = \bar{m}_d$  herein, which is consistent with the theoretical estimates summarised in Ref. [15]. The results we report herein are qualitatively and quantitatively insensitive to halving or doubling this ratio.

Realistic DSE studies show that there are differences between the  $u$  and  $s$  quark propagators that cannot be accounted for simply by changing the mass in Eqs. (5) and (6). An example is the vacuum quark condensate, which, using the model quark propagator defined in Eqs. (5)-(6) and the definition in Ref. [10], is given by [3]:

$$\langle \bar{q}^f q^f \rangle_{\mu^2}^{\text{vac}} = -(2D)^{\frac{3}{2}} \left( \ln \frac{\mu^2}{\Lambda_{\text{QCD}}^2} \right) \frac{3}{4\pi^2} \frac{b_0^f}{b_1^f b_3^f} . \quad (15)$$

The current theoretical prejudice [21] is that  $\langle \bar{s}s \rangle^{\text{vac}} \sim (0.5 - 0.8) \langle \bar{u}u \rangle^{\text{vac}}$ . We have explored the response of our calculated kaon observables to variations in  $\langle \bar{s}s \rangle$ . We believe that the sensitivity is too weak to provide a robust, independent estimate of  $\langle \bar{s}s \rangle$ . However, our calculations favour larger values and hence in the calculations reported herein we used  $\langle \bar{s}s \rangle^{\text{vac}} = 0.8 \langle \bar{u}u \rangle^{\text{vac}}$ , which was implemented by setting

$$b_0^s = 0.8 b_0^u , \quad b_1^s = b_1^u , \quad b_3^s = b_3^u . \quad (16)$$

To allow for a minimal residual difference between the  $u$  and  $s$  quark propagators we did not allow  $C_{\bar{m}_s}^s$  to vary, simply setting

$$C_{\bar{m}_s}^s = C_{\bar{m}_u}^u = 0 , \quad (17)$$

and allowed variations only in the parameter  $b_2^s$ . To provide for a difference between  $\Gamma_\pi$  and  $\Gamma_K$  we also allowed  $C_{m_s=0}^s \neq C_{m_u=0}^u$ .

Having fixed the  $u$ -quark parameters in the pion sector we then have a two-parameter extension of the model to the  $s$ -quark sector. These parameters are fixed by requiring that the model reproduce, as well as possible, the experimental values for the dimensionless quantities  $f_K/f_\pi = 1.22 \pm 0.02$ ,  $r_{K^\pm}/r_{\pi^\pm} = 0.88 \pm 0.07$  and  $m_K/f_K = 4.37 \pm 0.05$ .

The kaon mass is obtained by solving  $\Pi_K(P^2) = 0$  where

$$\begin{aligned} \Pi_K(P^2) = 8N_c \int \frac{d^4k}{(2\pi)^2} & \left( B_{m_s=0}^s(k^2) \sigma_{S_{m_s=0}}^s(k^2) - \right. \\ & \left. [B_{m_s=0}^s(k^2)]^2 [k_+ \cdot k_- \sigma_{V_{m_u \neq 0}}^u(k_+) \sigma_{V_{m_s \neq 0}}^s(k_-) + \sigma_{S_{m_u \neq 0}}^u(k_+) \sigma_{S_{m_s \neq 0}}^s(k_-)] \right), \end{aligned} \quad (18)$$

with  $k_+ = k + \alpha P$ ,  $k_- = k - \beta P$ . For  $P^2 + m_K^2 \simeq 0$ ,  $\Pi_K(P^2) \approx f_K^2 (P^2 + m_K^2)$  with

$$f_K^2 = \left. \frac{d}{dP^2} \Pi_K(P^2) \right|_{P^2 = -m_K^2}, \quad (19)$$

which also ensures the correct (unit) normalisation of the charged kaon form factor. These expressions are straightforward generalisations of Eqs. (11) and (12). Similar expressions are obtained in Ref. [23].

Following this procedure we obtain

$$C_{m_s=0}^s = 1.69, \quad b_2^s = 0.74. \quad (20)$$

With  $\bar{m}_u \neq \bar{m}_s$  the requirement  $F_{K^0}(Q^2 = 0) = 0$  entails  $\alpha = 0.49$  ( $\approx 1/2$ ). A comparison between calculation and experiment is presented in Table I. The calculated form factors are presented in Figs. 1 and 2.

The difference between the calculated and measured values of the charge radii and scattering lengths in Table I is a measure of the importance of final-state, pseudoscalar rescattering interactions and photon–vector-meson mixing, which are not included in generalised-impulse approximation [7]. Our calculation suggests that such effects contribute less than  $\sim 15\%$  and become unimportant for  $Q^2 > 1 \text{ GeV}^2$ . The fact that the calculated values of  $f_K/f_\pi$  and  $r_K/r_\pi$  agree with the experimental values of these ratios suggests that such effects are no more important for the kaon than for the pion.

**4. Summary and Discussion.** We find that on the range of  $Q^2$  currently accessible to experiment  $F_{K^\pm}(Q^2) > F_\pi(Q^2)$ . This is qualitatively consistent with Ref. [24], however, our calculated results, for both form factors, are uniformly smaller in magnitude; as is the difference between them. The peak in  $Q^2 F(Q^2)$ , which is most pronounced for the  $K^\pm$ -meson, is a signal of quark-antiquark recombination into the final state meson in the exclusive elastic scattering process.

For  $Q^2 > 3 \text{ GeV}^2$  we have  $F_{K^\pm}(Q^2) < F_\pi(Q^2)$  but the difference is small and sensitive to the form of the kaon Bethe-Salpeter amplitude. The behaviour of  $F_{K^\pm}(Q^2)$  at  $Q^2 > 2 \sim 3 \text{ GeV}^2$  is influenced by details of the Ansatz for the kaon Bethe-Salpeter amplitude, Eq. (9), that are not presently constrained by data. The results obtained for  $Q^2 < 2 \text{ GeV}^2$  are not

sensitive to details of our parametrisation. We therefore view the results for  $Q^2 > 2 \text{ GeV}^2$  with caution.

These observations emphasise that measurement of the electromagnetic form factors is a probe of the bound state structure of the meson; i.e., its Bethe-Salpeter amplitude.

For the neutral kaon  $r_{K^0}^2 < 0$  and  $F_{K^0}(Q^2)$  is similar in form and magnitude to the charge form factor of the neutron. The fact that  $F_{K^0}(Q^2) \neq 0$  is a manifestation of the  $u$ - $s$  mass difference. We note that charge conjugation symmetry ensures  $F_{\pi^0}(Q^2) \equiv 0$ .

Our calculated results are not sensitive to changes in the  $m_s$  in the range  $m_s/m_{\text{ave}} \in [15, 30]$  nor to changes in  $\langle \bar{s}s \rangle$  in the range  $\langle \bar{s}s \rangle / \langle \bar{u}u \rangle \in [0.5, 1.0]$ . Nevertheless, the requirement that the calculation reproduce known values of kaon observables does lead to differences between the  $u$ - and  $s$ -quark propagators. This emphasises that measurement of the form factors is also a probe of nonperturbatively generated differences between the  $u$ - and  $s$ -quark propagation characteristics.

**Acknowledgments.** We acknowledge useful conversations with A. J. Davies. This work was supported by the National Science Foundation under grant no. INT92-15223; the Australian Research Council under grant no. S02947481; and the US Department of Energy, Nuclear Physics Division, under contract number W-31-109-ENG-38. The calculations described herein were carried out using the resources of the National Energy Research Super-computer Center.

## REFERENCES

- [1] CEBAF experiment E-91-016, Spokesperson: B. Zeidman; CEBAF experiment E-93-018, Spokesperson O. K. Baker; R. Magahiz et al., Letter of Intent, CEBAF PAC 9.
- [2] C. D. Roberts and A. G. Williams, Prog. Part. Nucl. Phys. **33** (1994) 477.
- [3] C. D. Roberts, in “Chiral Dynamics: Theory and Experiment”, A. M. Bernstein and B. R. Holstein (Eds.), Lecture Notes in Physics, Vol 452, p. 68 (Springer, Berlin 1995).
- [4] Z. Dong, H. J. Munczek and C. D. Roberts, Phys. Lett. B **333** (1994) 536; A. Bashir and M. R. Pennington, Phys. Rev. D **50** (1994) 7679.
- [5] R. Delbourgo and M. D. Scadron, J. Phys. G **5** (1979) 1621.
- [6] R. Dashen, Phys. Rev. **183**, 1245 (1969).
- [7] R. Alkofer, A. Bender and C. D. Roberts, Intern. J. Mod. Phys. A. **10** (1995) 3319.
- [8] M. R. Frank and P. C. Tandy, Phys. Rev. C **49** (1994) 478.
- [9] C. J. Burden, C. D. Roberts and A. G. Williams, Phys. Lett. **B285** (1992) 347.
- [10] A. G. Williams, G. Krein and C. D. Roberts, Ann. Phys. (NY) **210** (1991) 464.
- [11] M. R. Frank and C. D. Roberts, “Model gluon propagator and pion and rho-meson observables”, Preprint ANL-PHY-8072-TH-95 and INT95-00-97, 1995; to appear in Phys. Rev. C.
- [12] M. R. Frank, Phys. Rev. C **51** (1995) 987.
- [13] J. S. Ball and T.-W. Chiu, Phys. Rev. D **22** (1980) 2542.
- [14] R. Alkofer and C. D. Roberts, “Calculation of the anomalous  $\gamma\pi^* \rightarrow \pi\pi$  form factor”, Preprint numbers: ANL-PHY-8214-TH-95; UNITU-THEP-15/1995 (1995).
- [15] Particle Data Group, Phys. Rev. D **50** (1994) 1173.
- [16] S. R. Amendolia, *et al*, Nucl. Phys. B **277** (1986) 168.
- [17] S. R. Amendolia, *et al*, Phys. Lett. B **178** (1986) 435.
- [18] W. R. Molzon, *et al.*, Phys. Rev. Lett. **41** (1978) 1213.
- [19] C. D. Roberts, R. T. Cahill, M. E. Sevier and N. Iannella, Phys. Rev. D **49** (1994) 125; D. Pocanić, in “Chiral Dynamics: Theory and Experiment”, A. M. Bernstein and B. R. Holstein (Eds.), Lecture Notes in Physics, Vol 452, p. 95 (Springer, Berlin 1995); M. E. Sevier, *ibid*, p. 114.
- [20] C. J. Burden, Lu Qian, C. D. Roberts, P. C. Tandy and M. J. Thomson, work in progress.
- [21] S. Narison, “QCD Spectral Sum Rules” (World Scientific, Singapore, 1989) and references therein.
- [22] E. B. Dally, *et al.*, Phys. Rev. Lett. **45** (1980) 232.
- [23] P. C. Tandy, private communication.
- [24] W. W. Buck, R. A. Williams and H. Ito, Phys. Lett. B **351** (1995) 24.



TABLES

	Calculated	Experiment
$f_\pi$	0.0924 GeV	$0.0924 \pm 0.001$
$f_K$	0.113	$0.113 \pm 0.001$
$m_\pi$	0.1385	0.1385
$m_K$	0.4936	0.4937
$m_{1\text{GeV}^2}^{\text{ave}}$	0.0051	0.0075
$m_{1\text{GeV}^2}^s$	0.128	$0.1 \sim 0.3$
$-\langle \bar{u}u \rangle_{1\text{GeV}^2}^{\frac{3}{3}}$	0.221	0.220
$-\langle \bar{s}s \rangle_{1\text{GeV}^2}^{\frac{3}{3}}$	0.205	$0.175 - 0.205$
$r_{\pi^\pm}$	0.56 fm	$0.663 \pm 0.006$
$r_{K^\pm}$	0.49	$0.583 \pm 0.041$
$r_{K^0}^2$	-0.020 fm <sup>2</sup>	$-0.054 \pm 0.026$
$g_{\pi^0\gamma\gamma}$	0.505 (dimensionless)	$0.504 \pm 0.019$
$F^{3\pi}(4m_\pi^2)$	1.04	1 (Anomaly)
$a_0^0$	0.17	$0.21 \pm 0.01$
$a_0^2$	-0.048	$-0.040 \pm 0.003$
$a_1^1$	0.030	$0.038 \pm 0.003$
$a_2^0$	0.0015	$0.0017 \pm 0.0003$
$a_2^2$	-0.00021	
$f_K/f_\pi$	1.22	$1.22 \pm 0.01$
$r_{K^\pm}/r_{\pi^\pm}$	0.87	$0.88 \pm 0.06$

TABLE I. A comparison between the low-energy  $\pi$  and  $K$  observables calculated using the parameters of Eqs. (13) and (20), with the constraints of Eqs. (14), (16) and (17), and their experimental values. The calculation of  $g_{\pi^0\gamma\gamma}$  is discussed in Ref. [3] and  $F^{3\pi}(4m_\pi^2)$  in Ref. [14]. The quoted “experimental” values of  $m_{1\text{GeV}^2}^{\text{ave}}$ ,  $m_{1\text{GeV}^2}^s$ ,  $\langle \bar{u}u \rangle_{1\text{GeV}^2}$  and  $\langle \bar{s}s \rangle_{1\text{GeV}^2}$  are representative of current theoretical estimates in other approaches. Actual experimental values are extracted mainly from Ref. [15];  $r_\pi$  is taken from Ref. [16];  $r_{K^\pm}$  from Ref. [17];  $r_{K^0}^2$  from Ref. [18], and the  $\pi$ - $\pi$  scattering lengths,  $a_J^I$ , are discussed in Ref. [19].

FIGURES

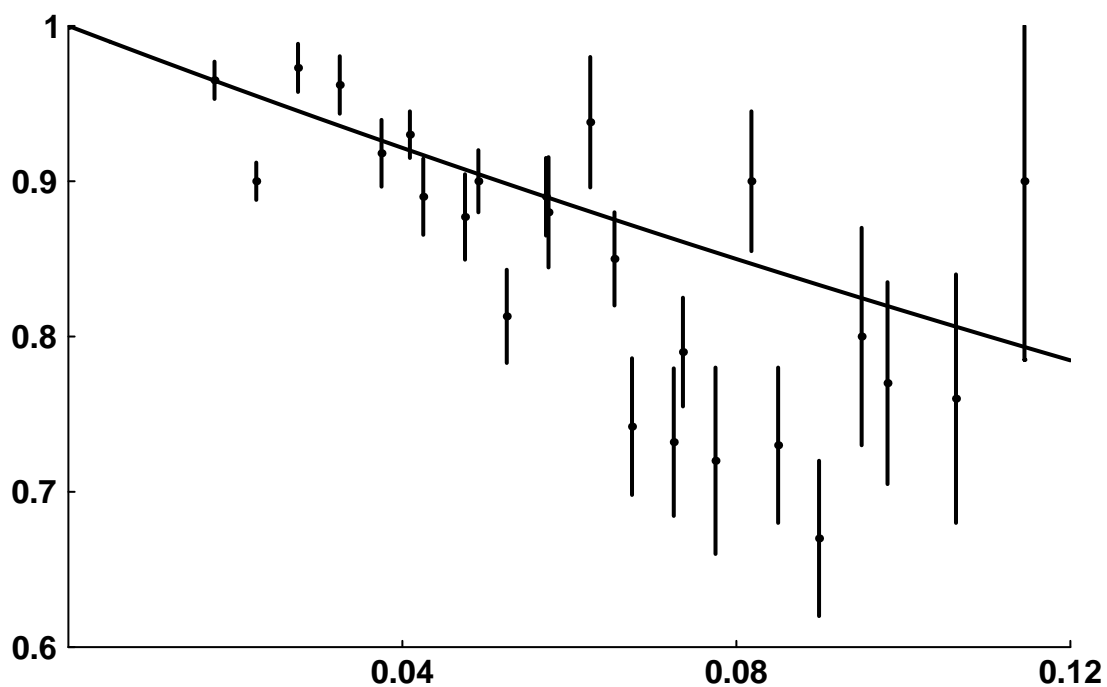


FIG. 1. Calculated form of  $F_{K^\pm}^2(Q^2)$  compared with the available data, which is taken from Refs. [17] and [22]. ( $Q^2$  is measured in  $\text{GeV}^2$ .)

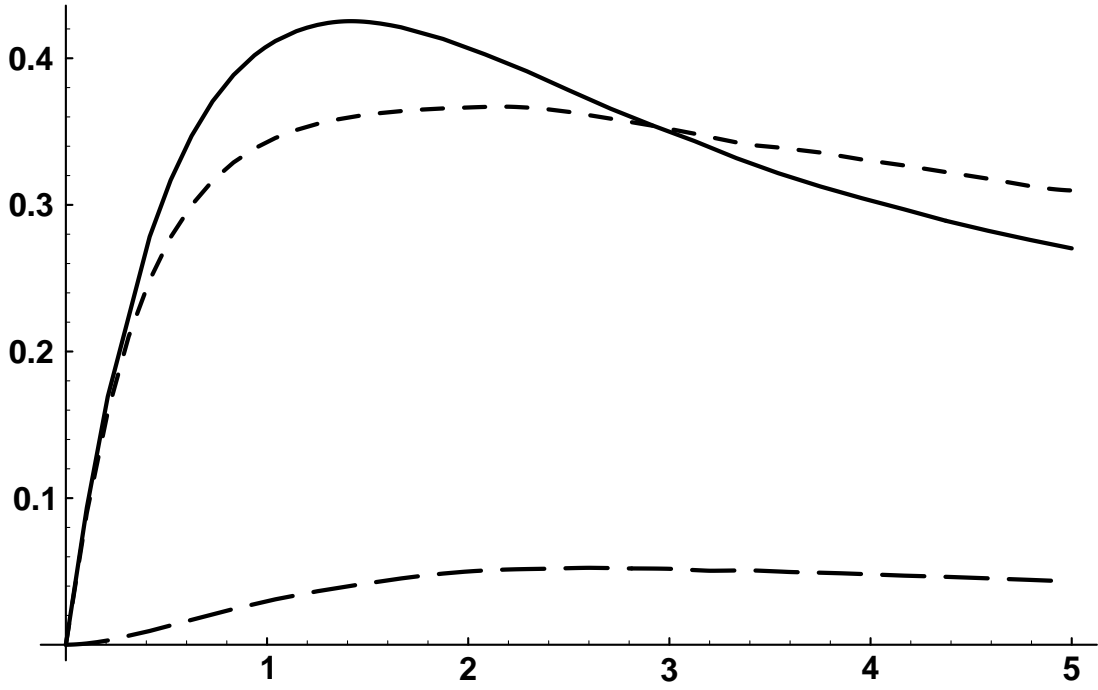


FIG. 2. Calculated form factors:  $Q^2 F_{K^\pm}(Q^2)$  - solid line;  $Q^2 F_{\pi^\pm}(Q^2)$  - short-dashed line;  $Q^2 F_{K^0}(Q^2)$  - long dashed line. ( $Q^2$  is measured in  $\text{GeV}^2$ .) The difference between  $F_{K^\pm}(Q^2)$  and  $F_{\pi^\pm}(Q^2)$  for  $Q^2 > 3 \text{ GeV}^2$  is small but is amplified in this figure because of the multiplication by  $Q^2$ .